Available online at www.sciencedirect.com
ScienceDirect
Journal of the European Ceramic Society 30 (2010) 271–275
www.elsevier.com/locate/jeurceramsoc

The study of $BiCr_xFe_{1-x}O_3$ thin films synthesized by sol–gel technique

Yuhua Zhang, Shengwen Yu *, Jinrong Cheng

School of Material Science and Engineering, Shanghai University, China

Available online 3 June 2009

Abstract

Cr-doped bismuth ferrite ($BiCr_xFe_{1-x}O_3$, BCFO) thin films were prepared by a sol–gel method with the value of x varying from 0 mol% to 10 mol%. The structures of the BCFO thin films were characterized by X-ray diffraction (XRD) and scanning electron microscopy (SEM) analysis was employed to represent the surface and cross-sectional morphologies of the thin films. Dielectric, electrical, ferroelectric and magnetic properties were measured by HP4294A, Keithley 4200, RT6000 and 6700 Magnet Controller at room temperature, respectively. The dielectric behaviour and insulation are improved in 3% Cr-doped BFO thin film which may be due to the reduced concentration of oxygen vacancies by 3% Cr doping.

Keywords: Films; Sol–gel process; X-ray methods; Electrical properties; Perovskites

1. Introduction

Multiferroic materials, which exhibit more than one ferroic property (ferroelectric, ferromagnetic, and ferroelastic),[1] are currently attracting extensive attentions due to their potential applications and fascinating physical phenomena.[2] However, multiferroic materials, including $TbMnO_3$,[3] $BiCrO_3$,[4] $DyMnO_3$,[5] rarely show multiferroic behaviours at room temperature (RT). Bismuth ferrite (BFO) is a rare single phase material which gives multiferroic characteristics at RT. BFO was discovered to show ferroelectric order with high Curie temperature T_C (~850 °C) and G-type antiferromagnetic order with Neel temperature T_N (~370 °C).[6] The structure of BFO is rhombohedrally distorted perovskite, which belongs to the space group $R3m$ with unit cell parameters $a = 3.962$ Å and $\alpha = 89.400°$.[7] The ferroelectricity of BFO material was reported to be ascribed to the stereochemically active of the Bi lone pair.[8]

Although bismuth ferrite material shows promising application potential on account of its coexistence of ferroelectric and antiferromagnetic properties at RT, some serious problems still need to be solved, such as high leakage current and weak ferromagnetism. Oxygen vacancy in BFO materials, which is mostly generated during the heat treatment, is the major origin in charge of the deterioration of insulation and the formation of Fe^{2+}, according to $V_O^X + 2Fe^{3+} \Leftrightarrow V_O^{\bullet\bullet} + 2\,Fe^{2+}$. Where $V_O^{\bullet\bullet}$ is oxygen vacancy and V_O^X is oxygen position. Following Le Chatelier principle, the concentration of Fe^{2+} would decrease if the content of Fe^{3+} is reduced. Therefore, doping at Fe site would suppress the formation of oxygen vacancies and reduce the concentration of Fe^{2+}. For example, Ti^{4+} and Zn^{2+} have been reported as the dopants substituting Fe^{3+} in BFO materials to lower leakage current.[9,10] However, some literatures also denote that substitution of ions with higher or lower valence for Fe^{3+} ions in BFO films would create cation vacancies or anion vacancies, respectively.[10] Upon the above, Cr^{3+} is considered as an appropriate candidate to substitute Fe^{3+} in $BiFeO_3$. Besides, the doping of Cr^{3+} ions is helpful in increasing the magnetic moment in BFO thin film due to the strong ferromagnetic coupling which exists between Fe^{3+} and Cr^{3+} under 180° superexchange interaction.[11] Moreover, the radii of Cr^{3+} (0.615 Å) is similar to Fe^{3+} (0.645 Å),[12] which indicates that the BFO structure could be less affected by light doping. Hence, Cr^{3+}-doped BFO thin films are going to be studied in this report.

2. Experimental method

The Cr-doped BFO (BCFO) thin films were fabricated on Pt/Si (1 1 1) substrates by a sol–gel method. Ferric nitrate $Fe(NO_3)_3{\cdot}9H_2O$, bismuth nitrate $Bi(NO_3)_3{\cdot}5H_2O$ and chromium nitrate $Cr(NO_3)_3{\cdot}9H_2O$ were adopted as raw materials, which were dissolved in 2-methoxyethanol (2-MOE), respectively. $Bi(NO_3)_3{\cdot}5H_2O$ and $Fe(NO_3)_3{\cdot}9H_2O$ were mixed as the precursor solution. The chromium nitrate $Cr(NO_3)_3{\cdot}9H_2O$

* Corresponding author at: 149 Yanchang Road, Box 32, Shanghai, 200072, China. Tel.: +86 21 56332704; fax: +86 21 56332694.
E-mail address: yusw@staff.shu.edu.cn (S. Yu).

0955-2219/$ – see front matter © 2009 Elsevier Ltd. All rights reserved.
doi:10.1016/j.jeurceramsoc.2009.05.005

was dissolved into the ready precursor solution, and then the catalyst acetic acid was added. The solutions with Cr^{3+} concentrations of 0%, 3%, 5% and 10% were prepared. These solutions were diluted to 0.2 M by adding 2-MOE and then stirred for 3 h at room temperature for the BCFO thin films synthesis. All solutions were prepared with excess 5% Bi to compensate the bismuth loss during annealing process. BCFO thin films were spin-coated onto Pt/Si (1 1 1) substrates at 3000 rpm for 25 s. Each layer was dried at 240 °C for 2 min on the hot plate, and then pyrolyzed at 400 °C for 10 min in a rapid thermal annealing under air condition. After depositing two layers, the amorphous films were annealed at 600 °C for 20 min. The above process was repeated three times to obtain the desired thickness.

Microstructures of the thin films were measured by X-ray diffraction (XRD, D/MAX-2550, Rigaku, Tokyo, Japan) at room temperature. The surfaces and morphologies of the films were checked by scanning electron microscopy (SEM, XL-30 FEG, Philips). In order to meet the requirement of measurement, Au top electrodes ($\Phi = 0.4$ mm) were fabricated on the film surface through a shadow mask. The electrodes were annealed at 300 °C for 20 min in order to get good contact between electrodes and films. Leakage currents and dielectric properties were measured by Keithley 4200 and HP 4294A impedance analyzer, respectively. Ferroelectric loops were tested by using RT6000 ferroelectric system (Radiant Technology, USA). Magnetic hysteresis measurements were performed on a quantum design physical property measurement system (6700 Magnet Controller). All tests were conducted at room temperature.

3. Results and discussion

The X-ray diffraction patterns for pure BFO (Cr 0%), 3% Cr-doped BFO (Cr 3%), 5% Cr-doped BFO (Cr 5%) and 10% Cr-doped BFO (Cr 10%) thin films are depicted in Fig. 1(a). The diffraction peaks are identified by PDF cards.[7] It is clear that no detectable impurity phases are observed in the films with Cr doping concentration varying from 0% to 3%. The splitting peaks of (1 1 0) and ($\bar{1}$ 1 0) can be distinguished in Fig. 1(b) which indicate the films are in rhombohedral structure. Nevertheless, in Cr 10%, the intensity of BFO peaks is much weaker than that of $Bi_7CrO_{12.5}$ which is a bothersome impurity phase. As shown in Fig. 1(b), the peaks of (1 1 0) and ($\bar{1}$ 1 0) of the films shift slightly due to the doping of Cr^{3+}. When the concentration of Cr^{3+} is 3%, the peaks shift to higher angle compared with Cr 0%, indicating a decrease of lattice parameter in Cr 3%. However, with further doping Cr^{3+}, the peaks shift to lower angle instead, which means the lattice parameters are increased alternately. The lattice parameters of the BCFO films are calculated to be 3.945 Å, 3.940 Å, 3.945 Å and 3.950 Å for Cr 0%, Cr 3%, Cr 5% and Cr 10%, respectively, which are less affected by the doping of Cr^{3+} ions. It may be due to the similar radii of Cr^{3+} and Fe^{3+} ions.

Fig. 2(a–h) is the SEM images of the surface and cross-sectional morphologies of Cr 0%, Cr 3%, Cr 5% and Cr 10%, respectively. The thicknesses of the thin films are 178 nm (Cr 0%), 200 nm (Cr 3%), 189 nm (Cr 5%) and 211 nm (Cr 10%). From these figures, it is convinced that the films are crack-free.

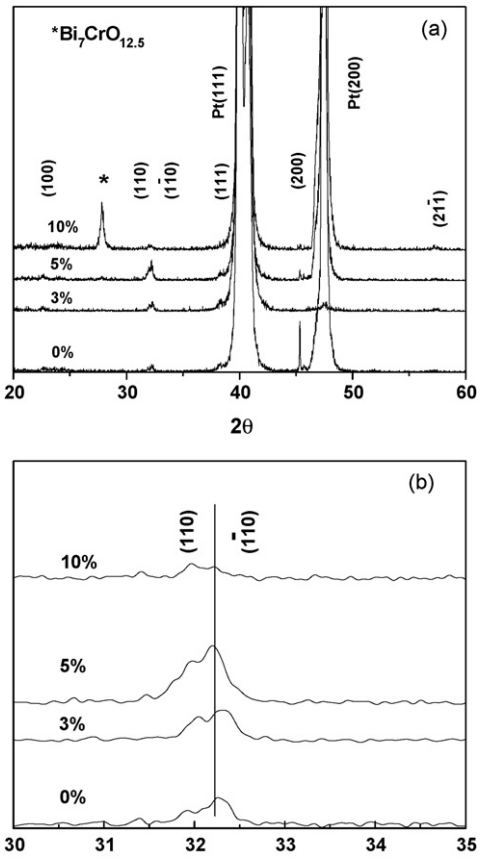

Fig. 1. (a) XRD patterns of Cr 0%, Cr 3%, Cr 5% and Cr 10% doped BCFO thin films, (b) the diffraction peaks corresponding to (1 1 0) and ($\bar{1}$ 1 0) of Cr 0%, Cr 3%, Cr 5% and Cr 10%.

When the concentration of Cr is 3%, the grain size is about 100 nm, which is smaller than that in Cr 0% (140 nm). With increasing of doping concentration, the grain sizes of Cr 5% and Cr 10% are growing to bigger than 120 nm. But more holes are found in Fig. 2(g) and (h), which means that the quality of BCFO thin films starts to get worse with further doping level (5% and 10%).

Fig. 3(a) is the frequency (1 kHz to 1 MHz) dependence of the dielectric constant (ε_r) and (b) is the corresponding dielectric loss at RT. The dielectric behaviours of the films do not exhibit strong frequency dependence except the dielectric loss of Cr 10%. According to the plots in Fig. 3(a), the dielectric constants of Cr 0%, Cr 3%, Cr 5% and Cr 10% are approximately 77, 82, 46 and 22 at 100 kHz, respectively. When the doping concentration is 3%, the dielectric constant reaches a maximum value and then decreases largely with further doping up to 10%. The dielectric losses of the BCFO thin films in Fig. 3(b) are all below 0.05 in the range of 1 kHz to 1 MHz except that of Cr 10%, which is much lower than others' work.[13,14] It is reported that low dielectric loss at low frequency would reflect low leakage current.[13] Therefore, it suggests that leakage current in Cr 3% might be the lowest while Cr 5% and Cr 10% would show poor insulation which could also be related to the impurity phase and roughness of surface morphologies.

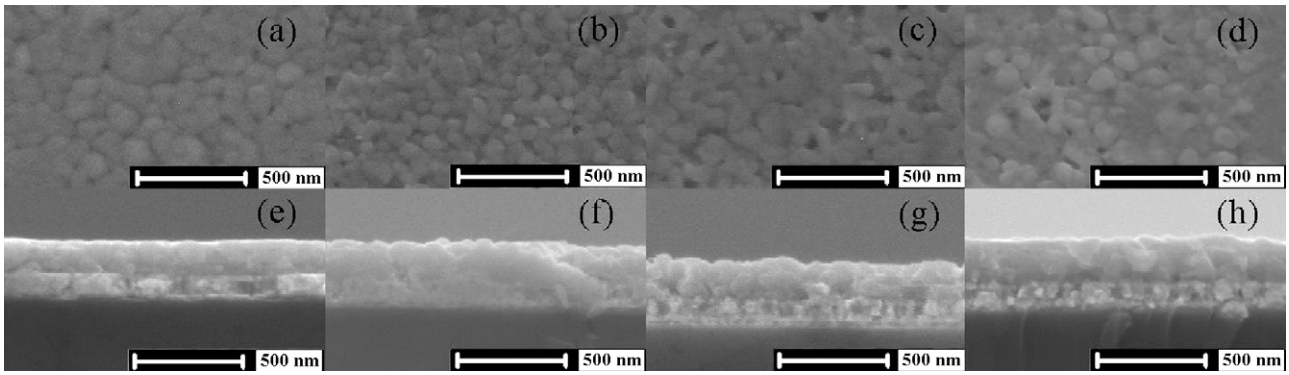

Fig. 2. SEM surface morphologies of BCFO films (a) Cr 0%, (b) Cr 3%, (c) Cr 5% and (d) Cr 10% and cross-sectional images of (e) Cr 0%, (f) Cr 3%, (g) Cr 5% and (h) Cr 10%.

According to the above analysis of dielectric response, the leakage current densities of Cr 0% and Cr 3% are characterized and shown in Fig. 4(a), which are in the order of 10^{-5} A/cm^2 and 10^{-6} A/cm^2 at 15 MV/m, respectively. As a result of light doping, it is evident that the value of leakage current in Cr 3% drops one order of magnitude at high electric field compared with Cr 0%, which means Cr 3% presents much improved insulation. Fig. 4(b) is the curves of ln J vs. $E^{1/2}$ and gives a slope of 0.0007 at relative low applied field for both thin films. It suggests that the high-frequency dielectric constant ε_∞ of the two films could be 4.41 if the conduction mechanism is Schottky emission or 16 for Poole–Frenkel emission. Since the ε_∞ of BFO is reported to be

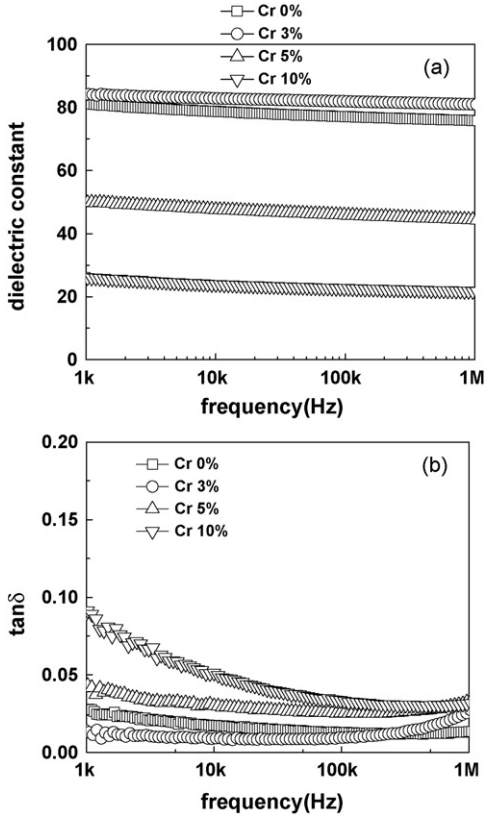

Fig. 3. (a) Dielectric constant of Cr 0%, Cr 3%, Cr 5% and Cr 10% and (b) the loss of Cr 0%, Cr 3%, Cr 5% and Cr 10% range from 1 kHz to 1 MHz.

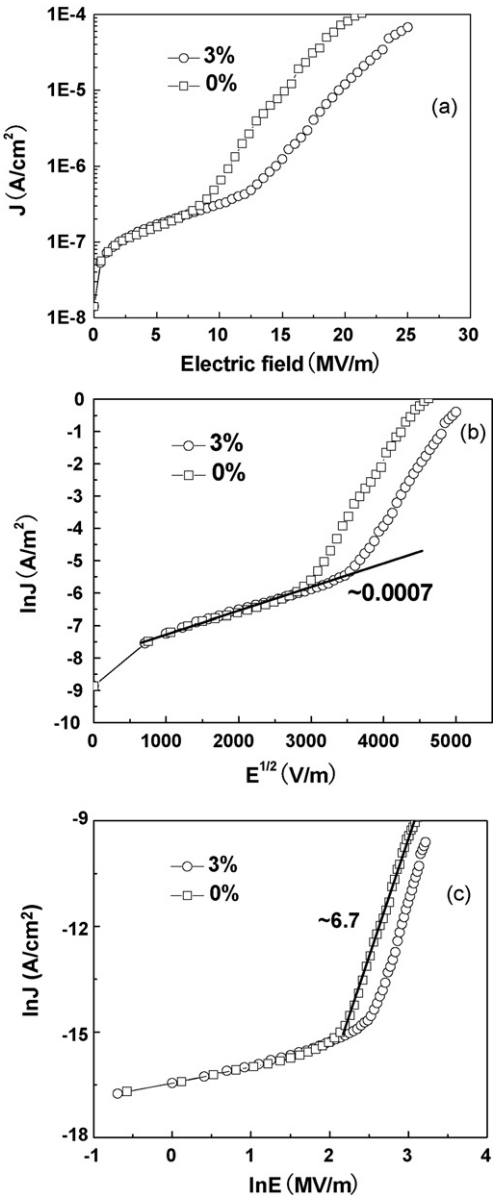

Fig. 4. (a) Leakage current density of Cr 0% and Cr 3%, (b) ln J vs. $E^{1/2}$ curves Cr 0% and Cr 3%, (c) ln J vs. ln E plot for Cr 0% and Cr 3%.

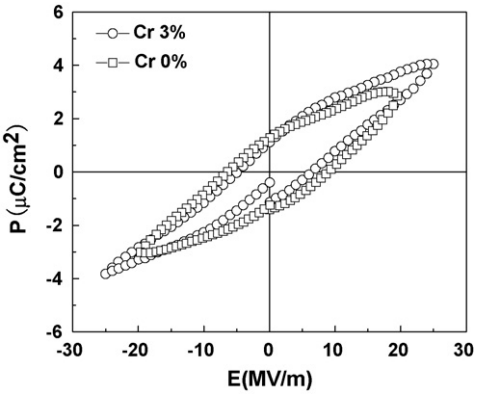

Fig. 5. Ferroelectric hysteresis loops of Cr 0% and Cr 3%.

about 6.25,[15] Schottky emission is assumed to be the dominant conduction mechanism at low electric field. In order to study the mechanisms of BFO at high electric field, the curves of ln J vs. ln E are plotted in Fig. 4(c). When the applied electric field reaches 7.8 MV/m for Cr 0% and 12 MV/m for Cr 3%, the slopes of the both curves abruptly rise to 6.7. This may be attributed to the trap charge limit (TCL) conduction. In this case, higher field is required for the Cr 3% thin film to behave the TCL conduction. It is deemed that the quasi-Fermi level locates in the trap distribution and the current is limited by trapped charges in TCL conduction.[16] In BFO based thin films, the possible trap center is Fe ions (Fe^{2+}).[15] When doping with Cr^{3+} ions, the concentration of oxygen vacancies may be reduced and the distribution of the shallow traps which are above the Fermi level may be correspondingly decreased. As a result, higher energy is demanded to activate the carriers to the conduction band from the deep traps which are below the Fermi level.

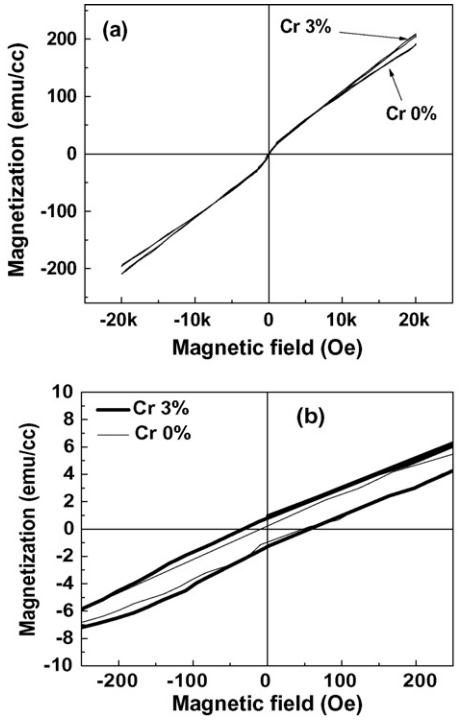

Fig. 6. (a) Magnetization (M–H) hysteresis loops of Cr 0% and Cr 3% and (b) the enlarged picture of (a).

The P–E hysteresis loops of Cr 0% and Cr 3% were also measured by using RT6000 of Radiant Technology at room temperature and shown in Fig. 5. P–E loops neither give saturated shapes, nor exhibit large remnant polarization, which are similar to some results of BFO thin films.[10] When the applied electric field is 20 MV/m for Cr 0% and 25 MV/m for Cr 3%, the $2P_r$ are both 2.3 μC/cm^2 and the $2E_c$ values are 15 MV/m and 11 MV/m, respectively. The shape of P–E loop can be seen improved by 3% Cr doping, which could be due to the improved insulation revealed by the characterization of leakage current.

Fig. 6 shows the magnetization (M–H) hysteresis loops of Cr 0% and Cr 3% thin films at room temperature. Weak ferromagnetic components are discovered in both thin films under low magnetic field. The weak ferromagnetism can be contributed to the nature of material and the absence of ferromagnetic impurity phases,[6] which consists with the results of XRD. $2M_r$ and $2H_c$ of Cr 3% and Cr 0% in Fig. 6(b) are approximate 2 emu/cm^3, 90 Oe and 1 emu/cm^3, 57 Oe, respectively. It shows that in spite of weak behaviour Cr 3% exhibits slightly clearer magnetic property than Cr 0%, which indicates Cr^{3+} doping could be helpful in increasing the magnetic moment.[11]

4. Conclusion

Perovskite $BiCr_xFe_{1-x}O_3$ ($x = 0$ mol%, 3 mol%, 5 mol%, and 10 mol%) thin films have been fabricated by sol–gel method. The dielectric behaviours of BCFO thin films are found being improved by light Cr^{3+} doping (3%), but deteriorated with further raising the doping level. The leakage current density of the Cr 3% doped thin film is reduced about 1 order of magnitude at high electric field, which may be due to the diminished concentration of oxygen vacancies and indicate a better resistivity. Subsequently, the shape of P–E hysteresis loop of Cr 3% is reasonably improved. In addition, both Cr 3% and Cr 0% thin films present weak magnetic property in the low magnetic field region and the magnetic property is slightly improved by 3% Cr doping.

Acknowledgments

This work was supported by Natural Science Foundation of Shanghai under Grant No. 08ZR1407700, Shanghai education committee foundation under Grant No. 07ZZ14, Shanghai Rising Star Program under Grant No. 08QH14008, Shanghai education development foundation under Grant No. 08SG41 and National Nature Science Foundation of China under Grant No. 50872080.

References

1. Setter, N., Damjanovic, D. and Eng, L., Ferroelectric thin films: review of materials, properties, and applications. *J. Appl. Phys.*, 2006, **100**, 051606.
2. Dawber, M., Rabe, K. M. and Scott, J. F., Physics of thin-film ferroelectric oxides. *Rev. Mod. Phys.*, 2005, **77**, 1083–1130.
3. Noda, K., Nakamura, S., Nagayama, J. and Kuwahara, H., Magnetic field and external-pressure effect on ferroelectricity in manganites: comparison between $GdMnO_3$ and $TbMnO_3$. *J. Appl. Phys.*, 2005, **97**, 10C103.

4. Kim, D. H., Lee, H. N., Varela, M. and Christen, H. M., Antiferroelectricity in multiferroic $BiCrO_3$ epitaxial films. *Appl. Phys. Lett.*, 2006, **89**, 162904.
5. Lee, J. H., Murugavel, P., Lee, D., Noh, T. W., Jo, Y., Jung, M.-H. *et al.*, Multiferroic properties of epitaxially stabilized hexagonal $DyMnO_3$ thin films. *Appl. Phys. Lett.*, 2007, **90**, 012903.
6. Kothari, D., Reddy, V. R., Gupta, A., Sathe, V., Banerjee, A., Gupta, S. M. *et al.*, Multiferroic properties of polycrystalline $Bi_{1-x}Ca_xFeO_3$. *Appl. Phys. Lett.*, 2007, **91**, 202505.
7. PDF 74-2016, Tomashpol'sky, Y.Y., Venevtsev, Y.N., Zhdanov, G.S., Kristallografiya, 1967.
8. Neaton, J. B., Ederer, C., Waghmare, U. V., Spaldin, N. A. and Rabe, K. M., First-principles study of spontaneous polarization in multiferroic $BiFeO_3$. *Phys. Rev. B*, 2005, **71**, 014113.
9. Hu, G. D., Fan, S. H., Yang, C. H. and Wu, W. B., Low leakage current and enhanced ferroelectric properties of Ti and Zn codoped $BiFeO_3$ thin film. *Appl. Phys. Lett.*, 2008, **92**, 192905.
10. Qi, X., Dho, J., Tomov, R., Blamire, M. G. and MacManus-Driscoll, J. L., Greatly reduced leakage current and conduction mechanism in aliovalent-ion-doped $BiFeO_3$. *Appl. Phys. Lett.*, 2005, **86**, 062903.
11. Chikazumi, S., Ohta, K., Adachi, K., Tsuya, N. and Ishikawa, Y., *Handbook of Magnetic Materials*. Asakura-syoten, Tokyo, 1975, p. 63 (in Japanese).
12. Shannon, R. D., Revised effective ionic radii and systematic studies of interatomic distances in halides and chaleogenides. *Acta Cryst.*, 1976, **A32**, 751–767.
13. Yun, K. Y., Noda, M., Okuyama, M., Saeki, H., Tabata, H. and Saito, K., Structural and multiferroic properties of $BiFeO_3$ thin films at room temperature. *J. Appl. Phys.*, 2004, **96**, 3399.
14. Yuan, G. L., Or, Siu Wing, Chan, Helen Lai Wa and Liu, Z. G., Reduced ferroelectric coercivity in multiferroic $Bi_{0.825}Nd_{0.175}FeO_3$ thin film. *J. Appl. Phys.*, 2007, **101**, 024106.
15. Pabst, G. W., Martin, L. W., Chu, Y. H. and Ramesh, R., Leakage mechanisms in $BiFeO_3$ thin films. *Appl. Phys. Lett.*, 2007, **90**, 072902.
16. Kang, H. S., Kim, K. H., Kim, M. S., Park, K. T., Kim, K. M., Lee, T. H. *et al.*, Electrical characteristics of light-emitting diode based on poly(p-phenylenevinylene) derivatives: CzEH-PPV and OxdEH-PPV. *Synth. Met.*, 2002, **130**, 279–283.